Available online at www.sciencedirect.com

ScienceDirect

Nuclear Physics A ••• (••••) •••–•••

NUCLEAR PHYSICS A

www.elsevier.com/locate/nuclphysa

# The Kuo–Brown effective interaction: From $^{18}$O to the Sn isotopes

Torgeir Engeland [a], Morten Hjorth-Jensen [b,c], Maxim Kartamyshev [a], Eivind Osnes [a,*]

[a] *Department of Physics, University of Oslo, N-0316 Oslo, Norway*
[b] *Department of Physics, Center of Mathematics for Applications, University of Oslo, N-0316 Oslo, Norway*
[c] *National Superconducting Cyclotron Laboratory, Department of Physics and Astronomy, Michigan State University, East Lansing, MI 48824, USA*

Received 14 March 2014; accepted 17 March 2014

This work is dedicated to the memory of Gerry Brown who played such a decisive role in defining the directions of nuclear physics throughout half a century, and who inspired so many students and colleagues

**Abstract**

After briefly reviewing the pioneering work on effective interactions by Gerry Brown and his group, and the developments which followed, we apply present-day effective interactions to large-scale shell-model calculations on the entire range of Sn isotopes from $^{102}$Sn to $^{132}$Sn. We have made explorative calculations starting from three different nucleon–nucleon potentials (Argonne V18, CD-Bonn, and N3LO) and evaluated the higher-order contributions to the effective interaction from both $G$-matrix and $V_{lowk}$ interactions. Further, we have checked the convergence of intermediate-state excitations up to $10\hbar\omega$ harmonic oscillator energy. Final extensive calculations were made of binding energies, excitation energies and B(E2) transition rates using an effective interaction based on a $G$-matrix evaluated from the chiral N3LO potential and including intermediate excitations up to $10\hbar\omega$ harmonic oscillator energy. The energy spectra are well reproduced throughout the region while overbinding of the ground states emerges as valence nucleons are added. The B(E2) rates agree well for the heavy isotopes, while they seem too low for the lighter ones.


*Keywords:* Effective interactions; Nuclear shell model; Excitation energies; Electromagnetic transition rates

* Corresponding author.

http://dx.doi.org/10.1016/j.nuclphysa.2014.03.012
0375-9474/

## 1. Introduction

After the independent-particle nuclear shell model was established around 1950, attempts were soon made to include interactions among the valence nucleons. In fact, the energy levels of light and medium-light nuclei were well described by employing simple phenomenological forces or by obtaining the interaction matrix elements by fitting the nuclear spectra. In particular, the latter method was successfully applied by Igal Talmi and collaborators [1]. They also obtained a simple benchmarking of the effective interaction. For example, they considered the Ca isotopes with $n$ interacting neutrons in the $0f_{7/2}$ orbital outside a closed $^{40}$Ca core. The ground-state energy of such a $j^n$ configuration is then

$$BE(j^n) = n\epsilon_j + \frac{1}{2}n(n-1)\alpha_j + \left[\frac{n}{2}\right]\beta_j, \tag{1}$$

where $[\frac{n}{2}]$ is the largest integer not exceeding $n/2$, $\epsilon_j$ is the single-particle energy, and $\alpha_j$ and $\beta_j$ are linear combinations of the two-particle interaction matrix elements $V_J \equiv \langle j^2 J|V|j^2 J\rangle$

$$\alpha_j = \frac{2(j+1)\overline{V}_{J>0} - V_0}{2j+1}, \qquad \beta_j = \frac{2(j+1)}{2j+1}(V_0 - \overline{V}_{J>0}), \tag{2}$$

where $\overline{V}_{J>0}$ is the angular momentum averaged interaction for $J > 0$. Empirically the quadratic term $\alpha$ was found to be small and repulsive (+0.23 MeV), whereas the pairing term $\beta$ was large and attractive (−3.33 MeV). Any prospective effective interaction in the Ca isotopes would thus have to be measured against these two parameters.

This would also apply to the so-called 'realistic' effective forces emerging in the 1960s. It was the ambition of Gerry Brown and his students at Princeton, Stony Brook and Copenhagen to derive an effective interaction from 'first principles', *i.e.*, a nucleon–nucleon interaction fitting the deuteron binding energy and the phase shifts of two-nucleon scattering. He expressed his point of view in characteristic terms at the Gatlinburg conference in 1966 [2]:

> "*Nuclear theorists have tended ... to hide the origin of the effective force behind a veil, to endow these origins with a 'Ding-an-sich' status, and to place them beyond the pale of inquiry. A privileged few are allowed to reach behind and pull out whatever components they need to explain particular phenomena. This is at least intellectually unsatisfying, and a number of us have tried hard in the past few years to make the connection between effective forces ... and the nucleon–nucleon force*."

## 2. The pioneering work in $^{18}$O

The first realistic potentials had a strong or infinitely strong repulsive core at short internucleon distances. The first step towards an effective interaction was then to get rid of the hard core by some renormalization procedure. This would lead to the Bethe–Brueckner reaction matrix $G$ [3]. However, $G$ alone was not sufficient to reproduce the nuclear spectra. Applied to $^{18}$O, as in the first work of Kuo and Brown [4], it gave insufficient ground-state binding and a compressed energy spectrum. In Ca the parameters $\alpha$ and $\beta$ were −0.21 and −0.66 MeV [5], compared to the empirical values quoted above of +0.23 and −3.33 MeV. It is essential to have $\alpha$ repulsive to open up the spectrum and $\beta$ sufficiently attractive to give enough binding.

The break-through came with the core-polarization term shown in Fig. 1a, where two valence nucleons interact via a particle–hole excitation of the core. This term was suggested by Bertsch

Please cite this article in press as: T. Engeland et al., The Kuo–Brown effective interaction: From $^{18}$O to the Sn isotopes, Nuclear Physics A (2014), http://dx.doi.org/10.1016/j.nuclphysa.2014.03.012

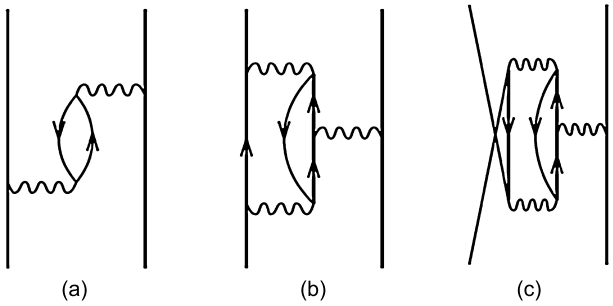


Fig. 1. The second-order core-polarization (a) and typical third-order (b, c) contributions to the effective interaction.

[6] and quantitatively evaluated by Kuo and Brown [4] and had the desired effect of increasing the ground-state binding and opening up the spectrum. The basic physical interpretation given by Gerry Brown was that while the reaction matrix $G$ was short range, the core polarization introduced a long-range quadrupole type interaction. In Ca the core polarization gave a repulsive contribution to the $\alpha$-parameter and an additional attractive contribution to the pairing term $\beta$, rendering $\alpha = 0.15$ MeV and $\beta = -1.96$ MeV [5].

## 3. Subsequent developments

### 3.1. Higher-order corrections

After the first successful derivation of a realistic effective interaction in $^{18}$O and $^{42}$Ca by Kuo and Brown several extensions followed. Barrett and Kirson [7] included third-order corrections such as diagrams (b) and (c) of Fig. 1 and found that these were typically of similar magnitude but opposite sign to the second-order contributions, thus indicating no obvious order-by-order convergence. Another development amounted to summing separate classes of diagrams to arbitrary order. For example, describing the core polarization in the Tamm–Dancoff or random-phase approximations [8] served to enhance the core–polarization contribution, while further inclusion of screening corrections to the particle–hole interaction recovered the second-order result [9]. Then, Kirson [10] performed a self-consistent nesting of vertices to arbitrary order, obtaining an induced particle–hole interaction which served to reduce the core–polarization effect substantially. A similar calculation was performed by Babu and Brown [11] in liquid $^3$He using a Green's function approach. Most of these calculations included virtual excitations (intermediate states) up to two oscillator shells. Vary, Sauer and Wong [12] found that high excitations due to the tensor force nearly wiped out the core-polarization term.

From third order on the perturbation expansion of the effective interaction contains so-called folded diagrams which correct for the fact that valence particles do not sit in valence orbits all the time. Such diagrams were included to arbitrary order by Kuo and collaborators [13] and have since been the basis of many derivations of the effective interaction, the present one included.

### 3.2. Many-particle shell-model calculations

The early applications of realistic effective interactions to shell-model calculations were restricted to systems with two or a few valence nucleons outside a closed-shell core. With the

Please cite this article in press as: T. Engeland et al., The Kuo–Brown effective interaction: From $^{18}$O to the Sn isotopes, Nuclear Physics A (2014), http://dx.doi.org/10.1016/j.nuclphysa.2014.03.012

advent of increased computing capacity and efficient algorithms, applications were made to increasingly larger systems. In the present paper we shall review calculations on the Sn isotopes.

## 4. Structure of the Sn isotopes

The Sn isotopes from $^{100}$Sn to $^{132}$Sn represent an outstanding testing ground for the many-particle shell model. Here, we consider up to 32 identical valence nucleons (neutrons) distributed among the $0g_{7/2}$, $1d_{5/2}$, $2s_{1/2}$, $1d_{3/2}$ and $0h_{11/2}$ orbitals outside a $^{100}$Sn closed-shell core. In the last two decades the experimental situation over the entire range of Sn isotopes is strongly improved and represents a crucial test to model calculations. In the early days only spectra of the stable isotopes mid-shell were known, but here realistic shell-model calculations were precluded because of inadequate computing power and algorithms. Thus, only calculations in the random-phase and BCS approximations with highly schematic forces could be done [14].

With vast improvements in both the experimental situation for the Sn isotopes and computing power, the entire range of Sn isotopes from $^{100}$Sn to $^{132}$Sn has become interesting as well as accessible to shell-model calculations. Separate studies have been made of the light [15] and heavy [16] Sn isotopes, starting from $^{100}$Sn and $^{132}$Sn cores, respectively. Here, we consider the entire region starting from a $^{100}$Sn core and using a more elaborate effective interaction obtained from more recent nucleon–nucleon forces.

The effective interaction used in the present work is evaluated in the folded-diagram approach of Kuo and collaborators [13], although to different approximations and using different nucleon–nucleon potentials, as further described below.

### 4.1. Large-scale shell-model calculation

For a given effective interaction $V_{eff}$ we solve the Schrödinger equation

$$(H_0 + V_{eff})|\Psi_k\rangle = E_k|\Psi_k\rangle \tag{3}$$

in the basis of all Slater determinants $|\Phi_\lambda\rangle$ for $n$ valence nucleons in the $0g_{7/2}$, $1d_{5/2}$, $0s_{1/2}$, $1d_{3/2}$ and $0h_{11/2}$ shell-model space:

$$|\Psi_k\rangle = \sum_{\lambda=1}^{d} C_\lambda^k |\Phi_\lambda\rangle, \tag{4}$$

$d$ being the dimension of the model space. The Slater determinants $|\Phi_\lambda\rangle$ are eigenfunctions of the one-body Hamiltonian $H_0$. We express these in the $m$-scheme, $m$ being the single-particle magnetic quantum number. Then, however, the dimensionality of the Hilbert space can be very large, up to 16 million for $n = 16$. On the other hand, using the $m$-scheme allows one to represent the individual Slater determinants by single computer words, such as

$$|\Phi_\lambda\rangle = \prod_{(jm)\in\lambda} a_{jm}^\dagger |0\rangle \longrightarrow (\underbrace{00111101010\cdots}_{32\ bits})_\lambda, \tag{5}$$

where the $n$ particles are distributed among the 32 different $jm$ states available in the chosen model space. Then, acting on these states by one- and two-particle operators $a_\alpha^\dagger a_\beta$ and $a_\alpha^\dagger a_\beta^\dagger a_\gamma a_\delta$ simply amounts to moving the particles around in the representation on the right hand side of the equation above.

Please cite this article in press as: T. Engeland et al., The Kuo–Brown effective interaction: From $^{18}$O to the Sn isotopes, Nuclear Physics A (2014), http://dx.doi.org/10.1016/j.nuclphysa.2014.03.012

To cope with such high dimensionality one needs special algorithms. We have chosen the Lanczos iteration procedure [15,17]. By this the effective Hamiltonian is transformed to a representation leading to a tri-diagonal energy matrix of low dimension which can easily be diagonalized. Starting with an arbitrary initial vector

$$|lanc_0\rangle = \sum_{k=1}^{d} A_k |\Phi_k\rangle, \tag{6}$$

where $A_k$ is some suitable amplitude at our choice, we employ a sequence of Lanczos type iterations

$$|lanc_{p+1}\rangle = H|lanc_p\rangle \tag{7}$$

to obtain a set of Lanczos vectors.

In each step $|lanc_{p+1}\rangle$ is orthogonalized to all previous ones. Finally we obtain a tri-diagonal energy matrix which can be diagonalized to give the lowest energy eigenvalues and eigenvectors with extremely good convergence properties. A good convergence criterion is obtained by evaluating the expectation value of the angular momentum $J$ for the calculated eigenstates. For example, in the present calculation of $^{116}$Sn we start with a basis of approximately $16 \cdot 10^6$ Slater determinants. In a Lanczos procedure with 200 iterations we obtain 10 eigenstates, all with angular momentum $J$ to four decimal points.

In constructing the energy Hamiltonian it is customary to use empirical single-particle energies, such that

$$H_0 = \sum_{jm} \epsilon_j a^{\dagger}_{jm} a_{jm}, \tag{8}$$

where the single-particle energies $\epsilon_j$ would be taken from the spectrum of $^{101}$Sn. However, only the ground state and the first excited state at 0.17 MeV are known. Furthermore, their spin assignments are ambiguous, being either $5/2^+$ or $7/2^+$ [18]. We have used the traditional choice of $5/2^+$ for the ground state and $7/2^+$ for the first excited state. In fact, the calculations are not very sensitive to the particular ordering of the two levels. To fix the remaining single-particle energies we had to rely on selected states of odd-A isotopes such as $^{109}$Sn and $^{111}$Sn. Again the results turned out to be only moderately sensitive to small variations in the single-particle energies. Finally, we used single-particle energies of 0, 0.20, 2.45, 2.55 and 3.00 MeV for the $1d_{5/2}$, $0g_{7/2}$, $2s_{1/2}$, $1d_{3/2}$ and $0h_{11/2}$ orbitals, respectively.

### 4.2. The effective interaction in various approximations

In the folded-diagram approach [13,19] the evaluation of the effective interaction is made in two steps. First the sum of all valence-linked non-folded diagrams is evaluated to give the so-called $\hat{Q}$-box interaction. Then, the folded diagrams are evaluated by folding the $\hat{Q}$-boxes into each other using generalized time ordering. Symbolically we may write

$$V_{\mathit{eff}} = \hat{Q} + \hat{Q} \int \hat{Q} + \hat{Q} \int \hat{Q} \int \hat{Q} + \cdots, \tag{9}$$

Please cite this article in press as: T. Engeland et al., The Kuo–Brown effective interaction: From $^{18}$O to the Sn isotopes, Nuclear Physics A (2014), http://dx.doi.org/10.1016/j.nuclphysa.2014.03.012

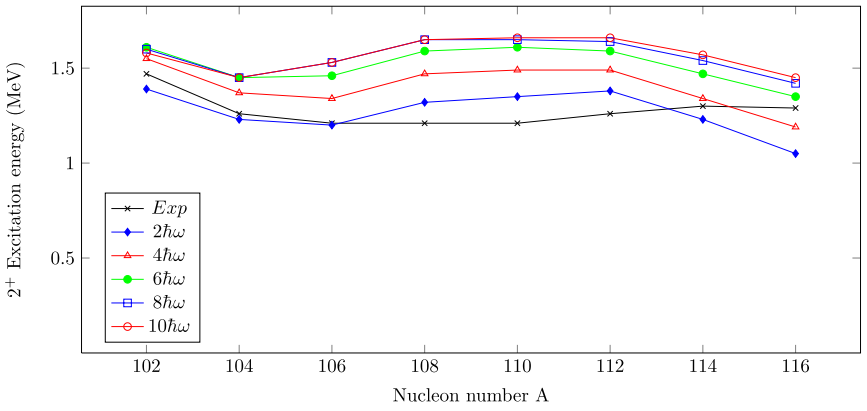


Fig. 2. The lowest $2^+$ level energy in $^{102-116}$Sn for the N3LO potential and $\hat{Q}$-boxes evaluated to third order and with intermediate excitations including up to $2\hbar\omega$, $4\hbar\omega, \ldots$ and $10\hbar\omega$ harmonic oscillator energy.

where $\int$ indicates folding by generalized time ordering. In the conjugate energy representation this amounts to taking energy derivatives of the $\hat{Q}$-boxes with respect to the starting energy $\omega$ in an iterative procedure:

$$V_{eff} = \lim_{i\to\infty} V_{eff}^{(i)}, \quad V_{eff}^{(i)} = \sum_{k=0}^{\infty} \frac{1}{k!} \frac{d^k \hat{Q}}{d\omega^k} V_{eff}^{(i-1)}. \tag{10}$$

Alternatively, one could use summation schemes for $V_{eff}$ such as the Lee–Suzuki method [20]. We have considered $\hat{Q}$-boxes evaluated to second and third order, with excitations from two to ten harmonic oscillator shells. At the basis of the $\hat{Q}$-box is the first-order term, which is the Bethe–Brueckner reaction matrix $G$. Besides $G$ we have also used $V_{lowk}$ (essentially a $T$-matrix) of Kuo and collaborators [21] as first-order term.

For the bare nucleon–nucleon interaction we have considered several choices, such as the $V_{18}$ of the Argonne group [22], the CD-Bonn potential [23] and the chiral N3LO potential [24].

### 4.3. The even Sn isotopes

Figs. 2 and 3 show two *explorative* calculations for the even isotopes from $^{102}$Sn to $^{116}$Sn. In Fig. 2 we show the energies of the first $2^+$ excited state for the N3LO potential and $\hat{Q}$-boxes evaluated to third order and with intermediate excitations from $2\hbar\omega$ to $10\hbar\omega$ harmonic oscillator energy. In Fig. 3 we show the first $2^+$ states with $\hat{Q}$ evaluated with intermediate excitations up to $10\hbar\omega$ for the three different nucleon–nucleon potentials mentioned above. These figures show (*i*) that the energy is fairly well converged by including up to $10\hbar\omega$ excitations, and (*ii*) that the $2^+$ energy is fairly independent of the basic nucleon–nucleon potential.

This being settled we calculated the low-energy spectrum for the entire range of even Sn isotopes from $^{102}$Sn to $^{130}$Sn. Fig. 4 shows the results for the lowest $2^+$ and $4^+$ states. Both the experimental and calculated $2^+$ energies are remarkably constant over the entire range of isotopes. It has been pointed out by Talmi [26] that this constancy of the $2^+$ energy throughout the region is indicative of the validity of generalized seniority. The calculated $0^+$ to $2^+$ spacing is slightly higher than the measured one and indicates that the pairing component of the effective interaction is somewhat too strong. Also the $4^+$ states show remarkable constancy over the range

Please cite this article in press as: T. Engeland et al., The Kuo–Brown effective interaction: From $^{18}$O to the Sn isotopes, Nuclear Physics A (2014), http://dx.doi.org/10.1016/j.nuclphysa.2014.03.012

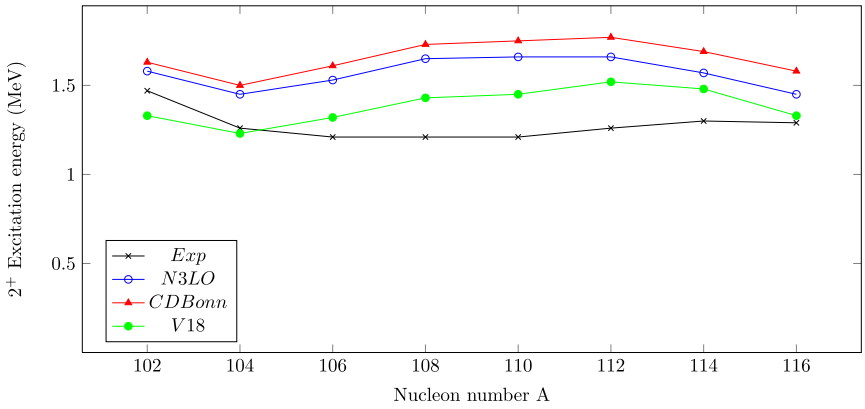


Fig. 3. The lowest $2^+$ level energy in $^{102-116}$Sn with $\hat{Q}$ evaluated to third order and intermediate excitations up to $10\hbar\omega$ with $G$-matrix for the three different nucleon–nucleon potentials.

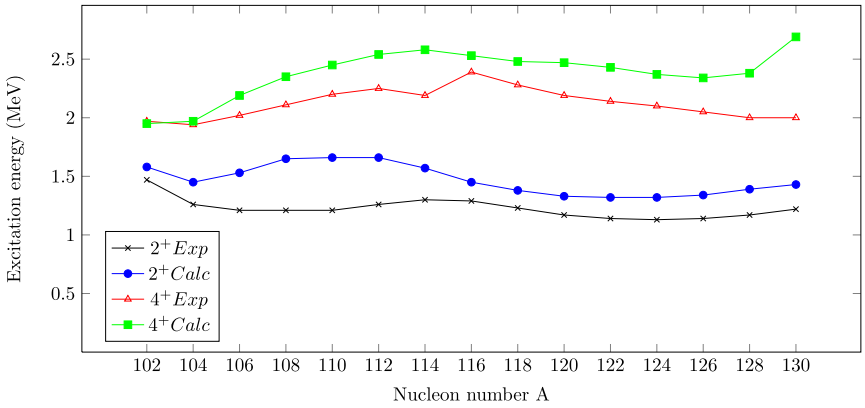


Fig. 4. The lowest $2^+$ and $4^+$ level energies in $^{102-130}$Sn with $\hat{Q}$ evaluated to third order and intermediate excitations up to $10\hbar\omega$ for the N3LO nucleon–nucleon potential. The experimental data are taken from Ref. [25].

of isotopes, although there are indications of shell effects. Shell effects are more pronounced for the $6^+$ state, not shown here.

Fig. 5 shows the $2^+$ and $4^+$ energies for $\hat{Q}$-boxes evaluated with $G$-matrix and $V_{lowk}$ interactions based on the N3LO and including up to $10\hbar\omega$ excitations. The level energies follow the same trend over the entire range of isotopes, although $V_{lowk}$ gives a larger spacing of the levels with respect to the ground state. The effective interaction based on $V_{lowk}$ shows similar convergence properties with respect to intermediate excitations as the $G$-matrix one shown in Fig. 2. It is worth noting from Fig. 6 that $V_{lowk}$ gives almost identical results for the three different nucleon–nucleon potentials considered, contrary to the situation for the $G$-matrix shown in Fig. 3. This indicates that the three different nucleon–nucleon potentials considered have slightly different off-shell components.

Fig. 7 shows binding energy calculations for $G$-matrix and $V_{lowk}$ based effective interactions using the N3LO potential. Both interactions overbind beyond $^{106}$Sn. The larger binding of $V_{lowk}$ reflects the stronger pairing component seen in the excitation spectra. We also include results of

Please cite this article in press as: T. Engeland et al., The Kuo–Brown effective interaction: From $^{18}$O to the Sn isotopes, Nuclear Physics A (2014), http://dx.doi.org/10.1016/j.nuclphysa.2014.03.012

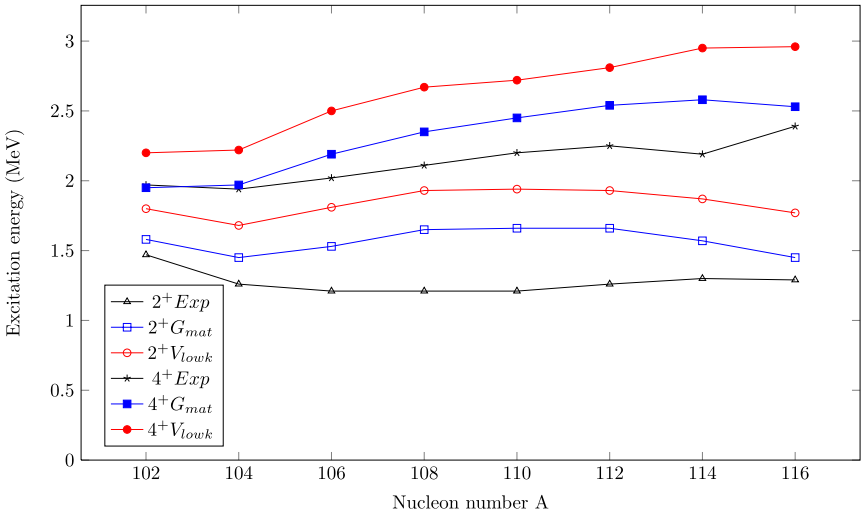


Fig. 5. The lowest $2^+$ and $4^+$ level energies in $^{102-116}$Sn with third-order $\hat{Q}$-boxes evaluated with $G$-matrix and $V_{lowk}$ interactions based on N3LO and including up to $10\hbar\omega$ excitations. The experimental data are taken from Ref. [25].

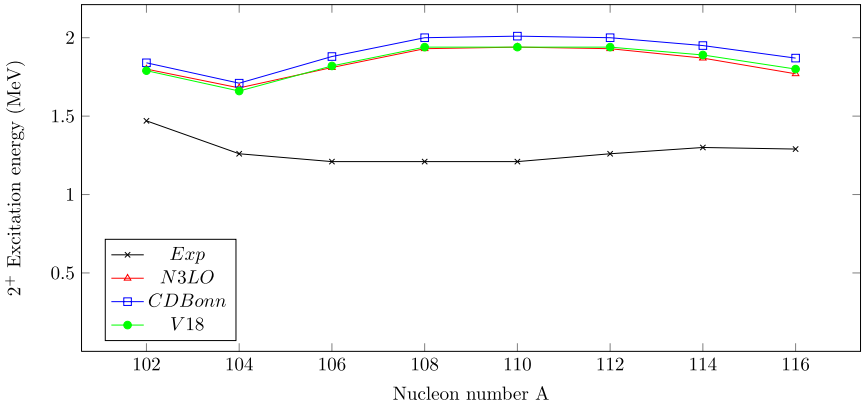


Fig. 6. The lowest $2^+$ level energy in $^{102-116}$Sn with $\hat{Q}$ evaluated to third order and intermediate excitations up to $10\hbar\omega$ with $V_{lowk}$ for three different nucleon–nucleon potentials.

the $2\hbar\omega$ case to indicate that it is necessary to include higher excitations to reduce the binding and to cause the curve to bend down.

In Fig. 8 we show the one-nucleon separation energy for N3LO and with $\hat{Q}$ evaluated to third order and $10\hbar\omega$ excitation. The lesser steepness of the calculated curves as compared to the empirical ones signals too much binding, due to insufficient repulsion in the average interaction. Adding a small repulsive component of less than 150 keV would align the two curves. It has been speculated that this might come from an effective three-body force resulting from the truncation of the shell-model space. In fact, the slight curvature of the curves indicates a small three-body component of the effective interaction, as also pointed out by Talmi [27]. In fact, the average three-body component deduced is minute, less than 10 keV. The distance between the even and odd curves measures the average pairing component of the effective interaction and is of similar

Please cite this article in press as: T. Engeland et al., The Kuo–Brown effective interaction: From $^{18}$O to the Sn isotopes, Nuclear Physics A (2014), http://dx.doi.org/10.1016/j.nuclphysa.2014.03.012

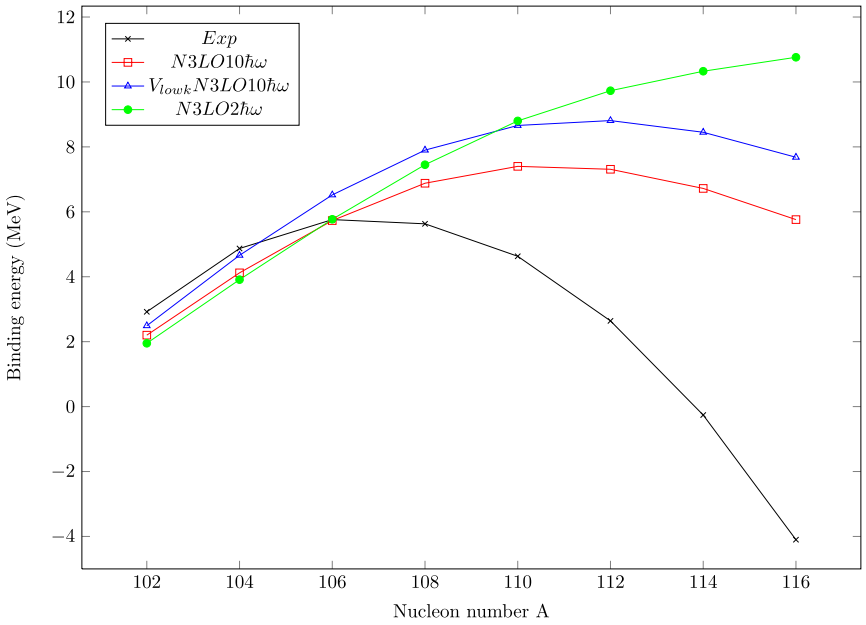


Fig. 7. Binding energies relative to $^{100}$Sn with third-order $\hat{Q}$-boxes evaluated with $G$-matrix and $V_{lowk}$ interactions based on the N3LO potential. The experimental data are taken from Ref. [25].

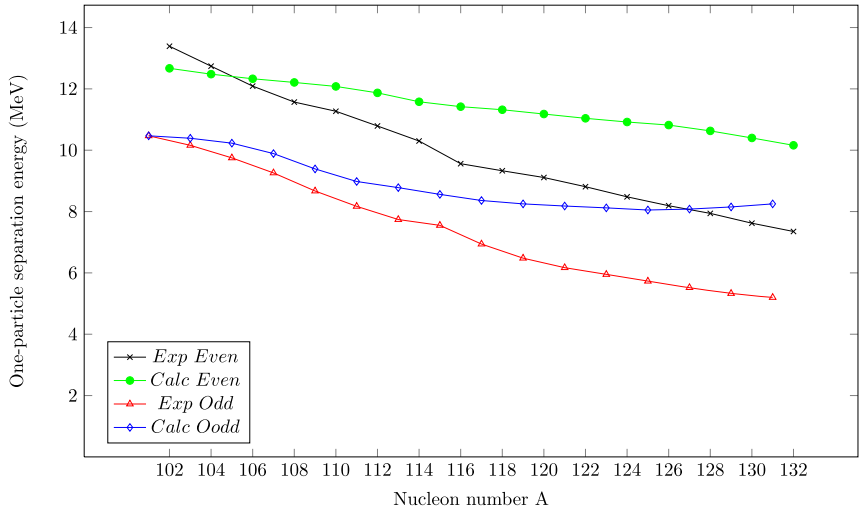


Fig. 8. Calculated and empirical one-particle separation energies for even and odd Sn isotopes. The calculations were made with a third-order $\hat{Q}$-box evaluated with an N3LO $G$-matrix and including up to $10\hbar\omega$ excitations. The experimental data are taken from Ref. [25].

size for the calculated and empirical curves, except in the middle of the shell where it is slightly overestimated by the calculations. If we apply Eq. (1) with $j$-independent coefficients $\alpha$ and $\beta$ to linear fits to the curves in Fig. 8, we find $\alpha = 0.21$ MeV and $\beta = -2.92$ MeV from the empirical

Please cite this article in press as: T. Engeland et al., The Kuo–Brown effective interaction: From $^{18}$O to the Sn isotopes, Nuclear Physics A (2014), http://dx.doi.org/10.1016/j.nuclphysa.2014.03.012

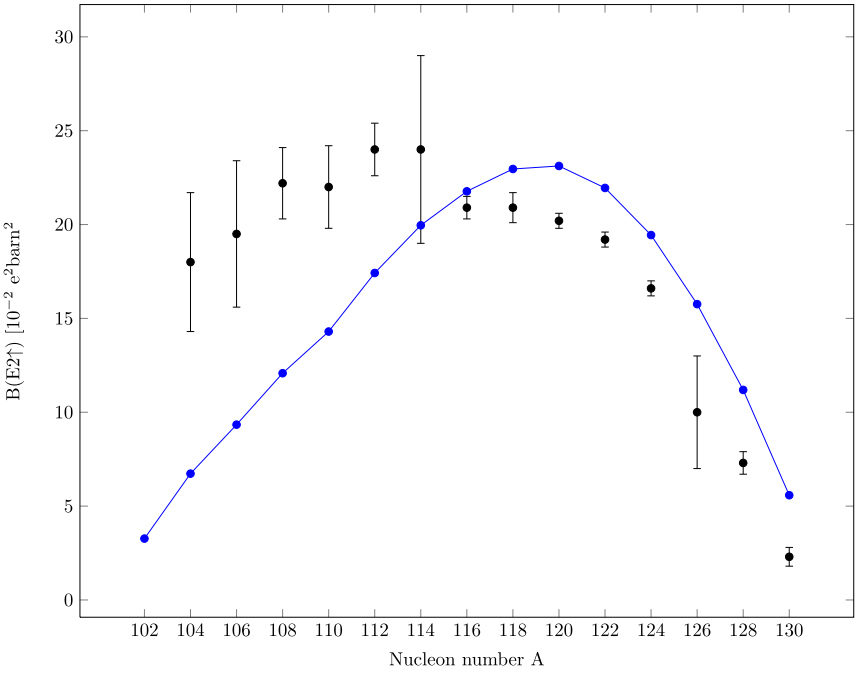


Fig. 9. Calculated and measured B(E2) values for the transition $0^+_{gs} \rightarrow 2^+_1$. The calculations were made with a third-order $\hat{Q}$-box evaluated with an N3LO $G$-matrix and including up to $10\hbar\omega$ excitations. An effective charge of $1.0e$ was used. The experimental data are taken from Ref. [28].

curves, and $\alpha = 0.08$ MeV and $\beta = -2.40$ MeV for the calculated ones. This is in line with what one finds in other regions of the nuclear chart.

To test the wave functions we calculated the B(E2) values for the transition $0^+_{gs} \rightarrow 2^+_1$. As seen in Fig. 9 the calculation reproduces well the measured rates for the heavier isotopes. For the lighter ones the calculated values are too low, and it has been speculated that proton excitations from the $^{100}$Sn core might contribute. There is, however, disagreement in the literature on both the measured values and the sizes of the error bars for the light isotopes, and more experimental work is clearly needed to resolve the question.

### 4.4. The odd Sn isotopes

For the odd isotopes we compare the calculated single-quasiparticle levels (*i.e.*, the ones with the largest generalized seniority one components) shown in Fig. 10 with the corresponding experimental ones shown in Fig. 11. There is fair agreement despite the uncertainty in the empirical single-particle energies. However, the assignment of empirical single-quasiparticle levels is uncertain, so one should only make a rough qualitative comparison. The agreement deteriorates towards the end of the shell. Thus, it is clear that a better experimental determination of the $^{101}$Sn single-particle levels is needed before one can draw firm conclusions.

Please cite this article in press as: T. Engeland et al., The Kuo–Brown effective interaction: From $^{18}$O to the Sn isotopes, Nuclear Physics A (2014), http://dx.doi.org/10.1016/j.nuclphysa.2014.03.012

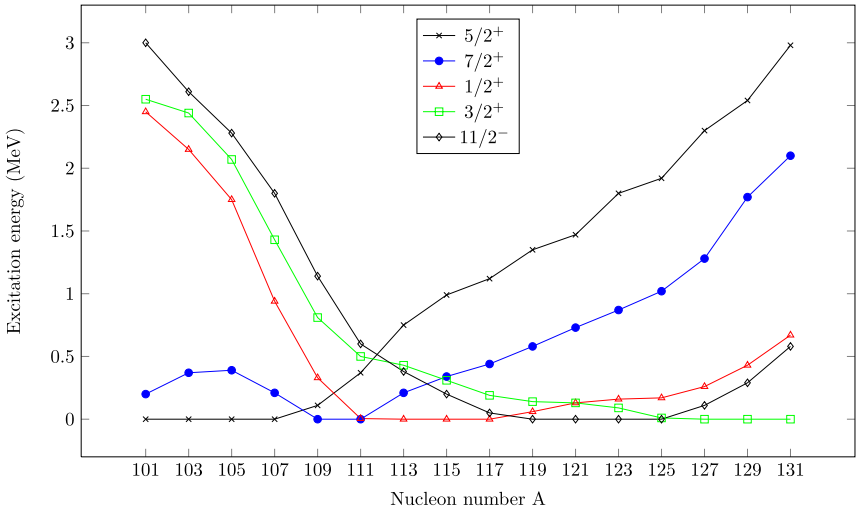


Fig. 10. Calculated single-quasiparticle levels throughout the Sn isotopes. The calculations were made with a third-order $\hat{Q}$-box evaluated with an N3LO $G$-matrix and including up to $10\hbar\omega$ excitations.

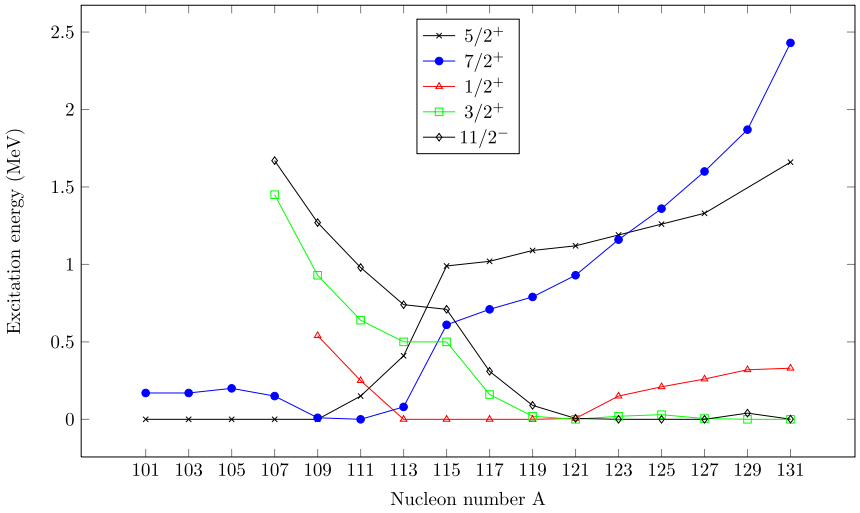


Fig. 11. Measured single-quasiparticle levels in the Sn isotopes. See the text for further explanation. The experimental data are taken from Ref. [25].

## 5. Summary and outlook

In this paper we have briefly reviewed the pioneering work by Kuo and Brown which led to their seminal effective interaction which proved so successful in shell-model calculations on nuclei near closed shells and initiated a very intense research activity giving rise to further extensions and refinements.

The aim of the present paper has been to apply state-of-art effective interactions to shell-model calculations on nuclei with a large number of valence nucleons. Thus we have studied the

Please cite this article in press as: T. Engeland et al., The Kuo–Brown effective interaction: From $^{18}$O to the Sn isotopes, Nuclear Physics A (2014), http://dx.doi.org/10.1016/j.nuclphysa.2014.03.012

spectroscopy of the entire range of Sn isotopes from $^{102}$Sn to $^{132}$Sn. This study has three objectives: (*i*) examine how well an effective interaction derived for two particles and single-particle energies extracted from the one-particle system is able to describe nuclear properties throughout the entire shell, (*ii*) establish the effective interaction by comparing different nucleon–nucleon potentials and approximation schemes, and (*iii*) use as large a shell-model space as possible. The effective interaction was evaluated in the folded-diagram approach using a $\hat{Q}$-box evaluated to third order. We made explorative calculations starting from three different nucleon–nucleon potentials (Argonne V18, CD-Bonn, and N3LO) and evaluated the higher-order contributions to the effective interaction from both $G$-matrix and $V_{lowk}$ interactions. Further, we have checked the convergence of intermediate-state excitations up to $10\hbar\omega$ harmonic oscillator energy. Final extensive calculations were made using an effective interaction based on a $G$-matrix evaluated from the chiral N3LO potential and including intermediate excitations up to $10\hbar\omega$ harmonic oscillator energy. The shell-model calculation was done by distributing up to 32 valence nucleons among the five single-particle orbitals $0g_{7/2}$, $1d_{5/2}$, $2s_{1/2}$, $1d_{3/2}$ and $0h_{11/2}$. This involves a large number of basis states, in the $m$-scheme as many as 16 million in the middle of the shell. To cope with such high dimensionality we used the Lanczos iteration procedure. In this procedure the effective Hamiltonian is transformed to a representation leading to a tri-diagonal energy matrix of low dimension which can easily be diagonalized.

The nuclear properties evaluated were ground-state binding energies with respect to the closed-shell core, separation energies, excitation energies and B(E2) values for the transition $0^+_{gs} \rightarrow 2^+_1$. The experimental spectra show nearly constant $2^+$ and $4^+$ spacings with respect to the ground state, indicating validity of generalized seniority. This is well reproduced by the calculations, although the $2^+$–$0^+$ spacing is on average 250 keV too big, reflecting that the pairing component of the effective interaction is too large. The ground-state binding energies agree well for nuclei with only few valence nucleons, while overbinding emerges as valence nucleons are added. This overbinding may be rectified by adding a modest repulsive monopole component to the interaction. Such a component may come from an effective three-body interaction arising from the truncation of the shell-model space. There is further evidence for this from the separation energies which show a slight deviation from linear behavior. The B(E2) rates agree well for the heavy isotopes, while they seem too low for the lighter isotopes. It has been speculated that protons excited out of the $^{100}$Sn core may be responsible for such an increase. On the other hand, the measured transition rates disagreeing with the calculations have large error bars, and their accuracy need to be improved.

The present study suggests several avenues for follow-up work. As the set of single-particle states used reflects the meager experimental information in low-mass Sn isotopes, it may be wise to start from the $^{132}$Sn core and use single-hole energies extracted from $^{131}$Sn. Further, it is of interest to see which effect effective three-body forces will have on the binding and excitation energies. To resolve the problem of B(E2) rates an opening-up of the $^{100}$Sn core might be a way out.

## References

[1] A. de-Shalit, I. Talmi, Nuclear Shell Theory, Academic Press, New York, 1963, p. 342ff.
[2] G.E. Brown, Effective forces in nuclei, in: R.L. Becker (Ed.), International Nuclear Physics Conference, Gatlinburg, 1966, Academic Press, New York, 1967, p. 1049ff.
[3] K.A. Brueckner, C.A. Levinson, H.M. Mahmoud, Phys. Rev. 95 (1954) 217;
H.A. Bethe, Phys. Rev. 103 (1956) 1353;
H.A. Bethe, J. Goldstone, Proc. R. Soc. Lond. A 95 (1957) 551.

Please cite this article in press as: T. Engeland et al., The Kuo–Brown effective interaction: From $^{18}$O to the Sn isotopes, Nuclear Physics A (2014), http://dx.doi.org/10.1016/j.nuclphysa.2014.03.012

[4] T.T.S. Kuo, G.E. Brown, Nucl. Phys. 85 (1966) 40.
[5] T.T.S. Kuo, G.E. Brown, Nucl. Phys. 114 (1968) 241.
[6] G.F. Bertsch, Nucl. Phys. 74 (1965) 234.
[7] B.R. Barrett, M.W. Kirson, Nucl. Phys. 148 (1970) 145.
[8] E. Osnes, C.S. Warke, Phys. Lett. B 30 (1995) 306.
[9] E. Osnes, T.T.S. Kuo, C.S. Warke, Nucl. Phys. A 168 (1971) 190.
[10] M.W. Kirson, Ann. Phys. (NY) 66 (1971) 62;
M.W. Kirson, Ann. Phys. (NY) 68 (1971) 556;
M.W. Kirson, Ann. Phys. (NY) 82 (1974) 345.
[11] S. Babu, G.E. Brown, Ann. Phys. (NY) 78 (1973) 1.
[12] J.P. Vary, P.U. Sauer, C.W. Wong, Phys. Rev. C 7 (1973) 1776.
[13] T.T.S. Kuo, E. Osnes, Folded-Diagram Theory of the Effective Interaction in Atomic Nuclei, Springer Lecture Notes in Physics, vol. 364, Springer, Berlin, 1990, and references therein.
[14] L.S. Kisslinger, R.A. Sorensen, Fys. Medd. Dan. Vid. Selsk. 32 (1960) 1;
T.T.S. Kuo, E.U. Baranger, M. Baranger, Nucl. Phys. 79 (1966) 513.
[15] T. Engeland, et al., Phys. Scr. T 56 (1995) 58.
[16] A. Holt, et al., Nucl. Phys. A 634 (1998) 41.
[17] C. Lanczos, J. Res. Natl. Bur. Stand. 45 (1950) 255;
R.R. Whitehead, et al., Adv. Nucl. Phys. 7 (1977) 123.
[18] I.G. Darby, et al., Phys. Rev. Lett. 105 (2010) 162502;
D.D. Dijulio, et al., Phys. Rev. C 86 (2012) 031302(R).
[19] M. Hjorth-Jensen, T.T.S. Kuo, E. Osnes, Phys. Rep. 261 (1995) 125.
[20] S.Y. Lee, K. Suzuki, Phys. Lett. B 91 (1980) 79;
K. Suzuki, S.Y. Lee, Prog. Theor. Phys. 64 (1980) 2091.
[21] S.K. Bogner, T.T.S. Kuo, L. Coraggio, Nucl. Phys. A 684 (2001) 432c.
[22] R.B. Wiringa, V.G.J. Stocks, R. Schiavilla, Phys. Rev. C 51 (1995) 38.
[23] R. Machleidt, et al., Phys. Rev. C 63 (2001) 024001.
[24] D.R. Entem, et al., Phys. Rev. C 68 (2003) 041001.
[25] Chart of Nuclides, National Nuclear Data, Center, BNL, USA, http://www.nndc.bnl.gov/chart/.
[26] I. Talmi, Nucl. Phys. A 172 (1971) 1.
[27] I. Talmi, Simple Models of Complex Nuclei, Harwood, Chur, 1993, p. 464ff.
[28] S. Raman, C.W. Nestor, P. Tikkanen, At. Data Nucl. Data Tables 78 (2001) 1;
A. Banu, et al., Phys. Rev. C 72 (2005) 061305(R);
A. Ekström, et al., Phys. Rev. Lett. 101 (2008) 012502;
V.M. Bader, et al., Phys. Rev. C 88 (2013) 051301(R).

Please cite this article in press as: T. Engeland et al., The Kuo–Brown effective interaction: From $^{18}$O to the Sn isotopes, Nuclear Physics A (2014), http://dx.doi.org/10.1016/j.nuclphysa.2014.03.012